INFLUENCE OF HEAT TREATMENT ON MECHANICAL PROPERTIES OF WELDED JOINTS OF AW 2099 ALLOY

MICHAELA LOPATKOVA, MILAN MARONEK, JOZEF BARTA, MATEJ PASAK
Slovak University of Technology in Bratislava, Faculty of Materials Science and Technology in Trnava
Slovakia
DOI: 10.17973/MMSJ.2022_10_2022097
michaela.lopatkova@stuba.sk

The paper is focused on the determination of the heat treatment effect on AW2099 welded joints properties. Laser beam welding was applied at constant welding parameters during the experiment. After the welding, solution annealing and artificial aging were applied at 150°C and 180°C for 24 hours. Subsequently, a static tensile test and microhardness measurement of welded joints were performed. The results of the tensile test showed that both heat treatment regimens resulted in an increase in the strength of welded joints and ensured an increase in hardness also in the area of the weld metal. The highest strength value (427.25MPa) was observed at a curing temperature of 150°C and a time of 24h.

KEYWORDS
AW 2099 alloy, laser beam welding, heat treatment, mechanical properties, artificial aging

1 INTRODUCTION

Compared to pure aluminium, aluminium-lithium alloys have a lower density, which is approximately 2560kg.m-3, while for other aluminium alloys the value is around 2700kg.m-3. The maximum solubility of lithium in aluminium is 6.5 wt.% (at 601°C) and decreases with decreasing temperature so that these aluminium alloys can be hardened [Moravčík et al. 2018].
Al-Li alloys have high fatigue strength, good toughness at low temperatures, high rigidity, resistance to fatigue crack growth, but limited ductility and low fracture toughness. Applications of these alloys are mainly in the aerospace industry, in military technology, or in the space industry [Michna et al. 2005; Joshi 2005].
The issue of heat treatment of these alloys is still under investigation, also because many of them, including AW2099, are relatively recently developed alloys, and it is assumed that other alloys with new interesting properties will continue to increase. Welding of aluminium, and its alloys are one of the more challenging tasks due to its properties. On atmospheric oxygen, a layer of alumina (Al2O3) is formed on the surface, which is electrically non-conductive and at the same time has a melting temperature approximately three times higher than pure aluminium. Aluminium has, among other things, high thermal conductivity and heat of fusion. All these properties complicate its weldability by conventional technologies [Bárta et al. 2008].

2 LITERATURE REVIEW

The influence of different solution annealing regimes on the mechanical properties of AW2099 alloy was investigated by Lin et al. (2014). In their experiment, the samples were subjected to a mechanical test after each solution annealing mode and the same curing mode. The solution annealing regimes were as follows: 520°C/1h; 530°C/1h; 540°C/1h; 540°C/4h; 550°C/1h, and 560°C/1h. After solution annealing, two-stage artificial aging was performed at 121°C/12h and 152°C/48h. In the experiment, it was shown that as the temperature of the solid solution increased, the number of primary elements in the alloy decreased and the degree of recrystallization increased significantly, leading to softening of the alloy. Dissolution of the primary particles of the solution during annealing led to the subsequent precipitation of the δ' and T1 phases in the aging process, which resulted in an increase in the strength of the alloy. The number of T1 phases increased to the maximum values during curing after solution annealing at 540°C, as no more copper-containing phases were dissolved at higher temperatures. At the same time, the higher solution annealing temperature caused a dramatic increase in the size as well as in the amount of recrystallized grains, which in turn softened the alloy. Experiments have shown that the long solution annealing time does not have a significant effect on the resulting mechanical properties of AW2099 alloy. The best results were obtained with a solution annealing regime of 540°C/1h, when the strength of the hardened alloy reached 604MPa and the elongation 7.9% [Lin et al., 2014].
Another experiment was performed by Wang et al. (2018), who investigated the welded joint of an Al-Cu-Li alloy welded by an electron beam. After welding, the samples were divided into three groups: 1) without heat treatment; 2) heat treatment with single-stage hardening of the alloy (solution annealing at 510°C/1h, quenching in water and aging at 155°C/16h) 3) heat treatment with double hardening (solution annealing at 510°C/1h, quenching in water, aging at 155°C/16h and aging at 130°C/12h. In the experiment, the microstructure, the courses of microhardness were monitored and a static tensile test was performed. For samples without heat treatment, the microstructure was similar to casting due to rapid solidification after welding. This microstructure was formed by equiaxed and dendritic grains. In the single-stage heat treatment, the microstructure showed an obvious change and consisted of approximately the same evenly distributed cellular grains. The dendritic structure was eliminated and a large number of dispersed particles precipitated in the grains. With two-stage aging, the result was even more advantageous as the structure was finer. From the static tensile test, it can conclude that the best results were obtained by 2-stage aging, which was predictable from the observation of the microstructure of the samples. In all cases, the test specimen was broken in the weld area, but a suitable heat treatment resulted in a value of 0.9 times the strength of the base material. Analogous to the results of the static tensile test, it can observe that the highest hardness in the weld metal was achieved by the material subjected to 2-stage aging. During this procedure, however, the hardness values increased not only in the weld area but also within the base material [Wang et al., 2018].
The use of highly concentrated energy sources for welding aluminium eliminates several problems arising from its physical and chemical properties. In the case of energy concentration in a narrow area, higher welding speeds can be used. Then, for example, even the high thermal conductivity of aluminium does not cause a serious problem, as the metal does not have as high heat dissipation from the weld site as with conventional welding technologies [Hrivnak, 2009].

Laser beam welding can be used on most aluminium alloys. When using a high welding speed, the porosity of the welds can occur, which may not only be due to the increased hydrogen content, but also due to the evaporation of some elements of the alloy. Another problem in laser welding of aluminium alloys can be the high reflection of aluminium, so it is necessary to use a beam with a high energy density, or to modify the surface by roughening or applying a thin film to increase the absorption of the beam. Welds can also be prone to hot cracking, especially for alloys with higher content of Cu and Mg, which are prone to form low-melting eutectics [Hrivnak, 2009].

3 METHODOLOGY

The performed experiment was focused on determining the influence of heat treatment on the mechanical properties of the AW2099 alloy after welding. The aim of the experiment was to determine the effect of the curing temperature during artificial aging on the resulting mechanical properties of the welded joints. The measured quantities were the yield strength, ultimate tensile strength, elongation and hardness, which were the results of a static tensile test and hardness measurement.

3.1 *Characteristics of the base material*

In the experiment, the investigated material was aluminium alloy AW2099, which belongs to the so-called third generation Al-Li alloys and was developed by Alcoa around 2003 [Rioja et al. 2012].
Dimensions of welded samples were 100x70x3mm. A thickness of 3mm was achieved by successive hot rolling from a thickness of 25.4mm after solution annealing (530°C/1h) and rapid cooling in water. The chemical composition and mechanical properties of the investigated alloy are summarized in Tab. 1 and 2.

	Chemical composition [wt.%]	
	min	max
Cu	2.40	3.00
Li	1.60	2.00
Zn	0.40	1.00
Mg	0.10	0.50
Mn	0.10	0.12
Zr	0.05	0.10
Ti	–	0.10
Fe	–	0.07
Si	–	0.05
Be	–	0.0001
Al	Bal.	Bal.

Table 1. Typical chemical composition of AW2099 [Smiths Metal Centers 2018]

Mechanical properties	Test direction	Value
Tensile strength [MPa]	In the rolling direction	500
	Perpendicular to the rolling direction	420
Yield strength [MPa]	In the rolling direction	350
	Perpendicular to the rolling direction	320
Elongation [%]	In the rolling direction	4.5
Modulus of elasticity in tension [GPa]		78

Table 2. Mechanical properties of AW2099 alloy [Smiths Metal Centers 2018]

3.2 *Welding method and parameters*

Welding was performed in Centre of Excellence 5-axis machining at Slovak University of Technology in Bratislava at Faculty of Materials Science and Technology in Trnava. The used welding method was laser beam welding. The source of the laser beam was a TruDisk 4002 disk laser (Fig. 1) with a laser head connected to a FANUC M-710ic / 50 robot (Fig. 2).

Figure 1. Laser welding center [MTF STU 2015]

Figure 2. 6-axis welding robot FANUC [MTF STU 2015]

In the present work, bead-on -plate welds were carried out. The preparation of the welded parts before the welding process consisted of grinding the surface on a surface grinder and a brush made of stainless steel. Next, the surface was cleaned with technical gasoline.
Argon was used as a shielding gas and helium was used as the forming gas to protect the weld pool and the weld area. The laser welding parameters used in the experiment are shown in Tab. 3.

Laser output power [W]	1700	
Welding speed [mm·s^{-1}]	15	
Focal point position	on surface	
Shielding gas [l·min^{-1}]	Surface	Ar/30
	Root	He/30

Table 3. Welding parameters

3.3 *Selection of heat treatment*

To determine the correct solution annealing time, samples of the base material were annealed in an air atmosphere oven at 540°C for 1, 2, 4 and 6 hours and quenched in water. The temperature for the solution annealing was selected based on the results of the [Wang et al. 2018].

Subsequently, the hardness was monitored over time on the sample's solution annealing, as shown in Fig. 3. The hardness measurement was performed on Zwick 3212 hardness tester by Vickers method under a load of 49.03N with the endurance time of 15 seconds. One hardness measurement was performed on the sample after each hour.

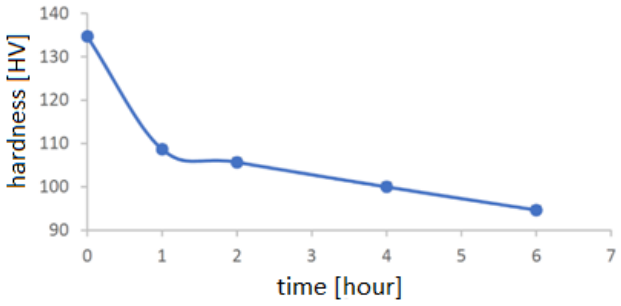

Figure 3. Dependence of hardness on the solution annealing time at 540°C

At the solution annealing time of approximately 1.5 hours, no further sharp decrease in hardness was observed. At longer times, there was only a slight decrease in hardness, which could have been caused by further grain growth. For this reason, the time for solution annealing was chosen 1.5h, which should be sufficient to dissolve all precipitates and form homogeneous solid alpha solution. Figure 4 shows images of the microstructure of the base materials as delivered and after solution annealing.

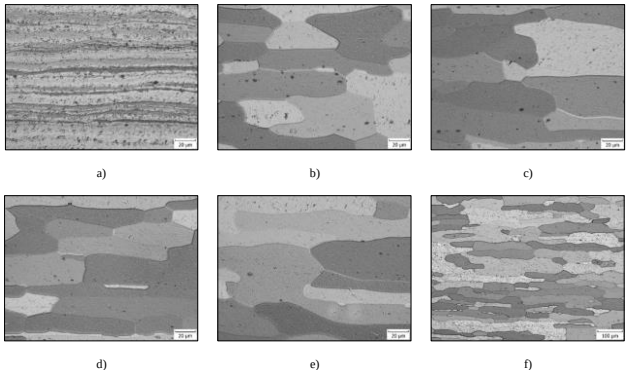

Figure 4. Microstructure of the base material after solution annealing at time: a) 0 h, b) 1 h, c) 2 h, d) 4 h, e) 6 h, f) 6 h (different magnification than other images)

In Figure 4a it is possible to observe base material (BM) without solution annealing (SA) and its texture after rolling. In Figures 4b - 4e it is possible to observe a significant increase in grain size after solution annealing at different times. At time 6h (Fig. 4e) it can be stated that the grain growth is clear compared to time 1h (4b). After solution annealing, 24 hours of artificial aging were performed at a curing temperature of 150°C and 180°C. For each artificial aging regime, 4 test rods were made for statistical processing of measured values.

4 RESULTS

In the experiment, AW2099 aluminium alloy materials were welded by laser welding parameters shown in Tab. 3.

After the welds were made, specimens for static tensile test were prepared using water jet to avoid thermal effects during cutting. Subsequently solution annealing and artificial aging in two modes were performed. After heat treatment, macroscopic and microscopic analysis, microhardness measurement and static tensile test were carried out.

4.1 *Visual inspection*

The performance of welds was evaluated by visual inspection according to the standard ISO 13919-2. The appearance of the welds is shown in Fig. 5. The width of the weld bead was approximately 4mm on the surface and 3mm at the root of the weld. The quality of the welds was satisfactory despite minor defects such as slight splashing on the surface or minor root fall.

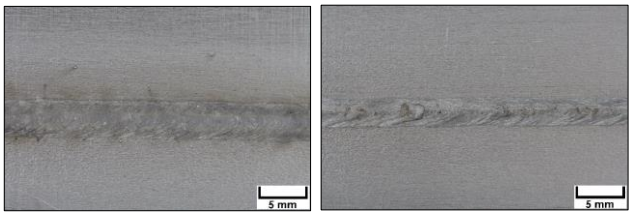

Figure 5. AW2099 alloy weld: a) weld surface b) weld root

4.2 *Macroscopic analysis*

Prior to macroscopic and microscopic analysis, the examined samples were prepared by conventional metallographic preparation consisting of wet grinding and polishing. Samples were polished on a Buehler VibroMet 2. Keller etchant (95ml H2O, 2.5ml HNO3, 1.5 HCl, 1ml HF) was used to reveal the microstructure. The etching time was approximately 10 seconds.

Figure 6 shows macro images of individual welds. In the case of a sample without heat treatment, the individual weld areas are not clearly visible in comparison with the heat-treated samples. In the case of the sample without heat treatment, the weld metal area was etched after a short time, but the heat-affected zone and the base material had not yet been etched at that time. On the heat-treated samples the individual areas of the base material are very clearly visible, heat-affected zone and transition to weld metal with columnar grains. In the Figures 6a and 6c, it is possible to observe the pores in the weld metal with the maximum size up to 50µm.

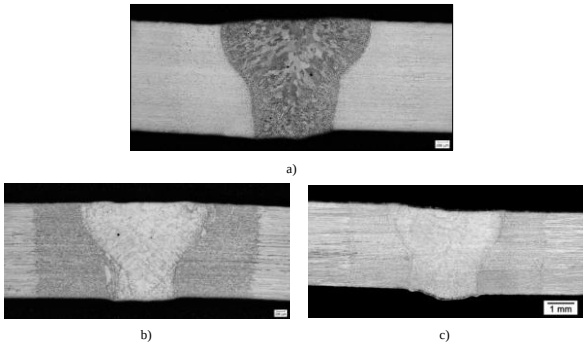

Figure 6. Macrostructure images of welded joints: a) without HT; b) 150°C/24h; c) 180°C/24h

Since the welding took place at the same parameters, the width of the individual weld areas was approximately the same. The width of the weld area together with HAZ reached 6-7mm, the width of the weld metal was 1-2mm at the root and 3mm at the surface. The HAZ area was 1-2mm wide on each side of the welded joint.

4.3 *Microscopic analysis*

Figure 7 represents a comparison of base materials after different HT modes at the same magnification. In the image of the base material without HT, it is possible to observe a certain undulation of the rolled grains and their deviation from the rolling direction by about 35°. The base material retained the original rolled grain structure even after recrystallization annealing.

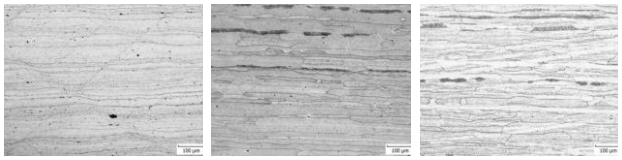

a) b) c)

Figure 7. Microstructure of BM: a) without HT; b) 150°C/24h; c) 180°C/24h. Source: own research

Figure 8 shows the transition from BM to HAZ, with recrystallization of grains occurring in HAZ. The grains in HAZ have a polyhedral character with the size from 10µm to 30µm.

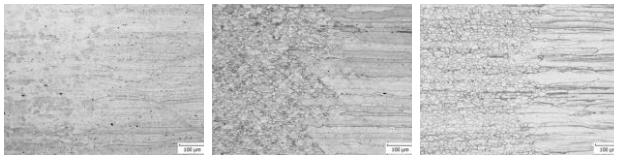

a) b) c)

Figure 8. Transition from BM to HAZ: a) without HT; b) 150°C/24h; c) 180°C/24h. Source: own research

Figure 9 documents the transition from HAZ to the WM area. On the border of these zones, it is possible to observe a fine-grained polyhedral structure with a grain size of 2 to 10µm. Towards the weld axis, the grains exhibit a columnar character, which is related to the direction of heat dissipation during solidification of weld metal.

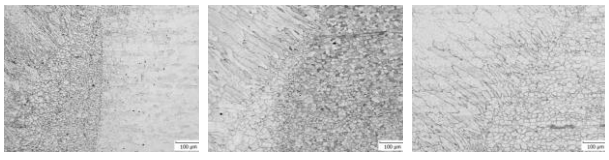

a) b) c)

Figure 9. Transition from HAZ to WM: a) without HT; b) 150°C/24h; c) 180°C/24h. Source: own research

The weld metal microstructure is documented in Fig. 10. Weld metal grains have a longitudinal character. Towards the weld axis, a dendritic structure can be observed in the weld metal. Dark areas appear along the grain boundaries and in the interdendritic areas, indicating the presence of precipitates.

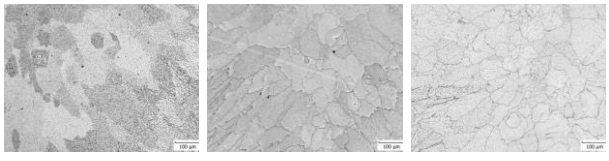

a) b) c)

Figure 10. Microstructure of WM: a) without HT; b) 150°C/24h; c) 180°C/24h. Source: own research

4.4 *Microhardness measurement*

The microhardness measurement was performed on an IndentaMet 1100 hardness tester under a load of 1 N with the endurance time of 10 seconds. The hardness was measured on the samples perpendicular to the weld axis from one side base material to another in two lines. One at a distance of 0.5mm below the weld surface and the other 0.5mm above the weld root. About 18 - 20 measurements were made on each sample below the surface and above the weld root. The number of measurements was determined so that at least 3 imprints were made on each side of the base material and the imprints were made at approximately the same distance from each other. A course was made from the measured values of hardness below the surface and above the root of the weld, which is shown in Fig. 11 and 12. In Figures 11 and 12, it can be seen that the highest hardness values were reached by the artificial aging regime, which was performed at a temperature of 150°C.

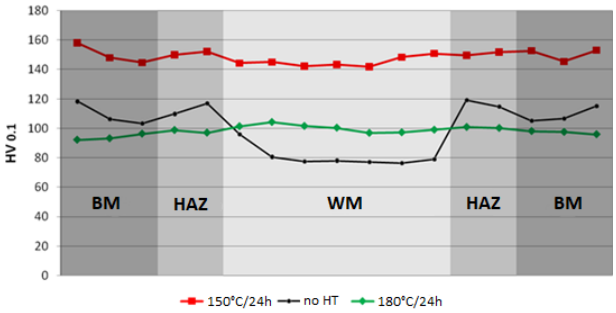

Figure 11. The course of microhardness under the weld surface

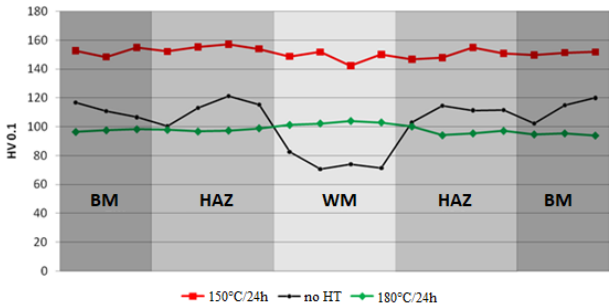

Figure 12. The course of microhardness over the root

From the measured values, the average hardness values of individual areas of welded joint were calculated and the standard deviation created from all measurements on a given sample, which is shown in Tab. 4.

	150°C/24h	180°C/24h	no HT
BM	150.92±3.05	95.81±1.61	110.58±5.48
HAZ	151.92±2.38	97.89±1.62	112.63±4.47
WM	146.31±3.36	101.05±1.89	78.37±4.38
SD	4.24	3.01	16.85

Table 4. Average hardness values of individual areas of welded joints for different HT modes/strategies
The legend: BM-base material; HAZ- heat affected zone; WM- weld metal, SD- standard deviation

The smallest variance of hardness values was achieved by the sample, which was cured at temperature 180°C. The largest variance was achieved by the unheated sample, where the hardness values in BM were significantly lower. The reason is mainly a sharp decrease in hardness in the area of BM.

HT mode	$\bar{R}p_{0.2}$-WM [MPa]	$\bar{R}p_{0,2}$- BM [MPa]	$\bar{R}$m-WM [MPa]	$\bar{R}$m-BM [MPa]	$\bar{A}$-WM [%]	$\bar{A}$-BM [%]	fracture in the weld
150°C/24h	390.00±2.5	412.00±4	427.25±8.75	459.00±6	3.16±1.87	11.88±0.05	4/4
180°C/24h	239.75±6.75	263.00±7	353.00±4.5	367.00±5	14.67±1.51	15.39±0.29	1/4
no HT	272.25±5.75	422.50±0.5	282.00±11.5	446.50±1.5	1.48±0,96	4.32±0.85	4/4

Table 5. Average values of mechanical properties for different HT modes/strategies

4.5 *Static tensile test*

The static tensile test of heat-treated bars was performed in accordance with standard EN 10002 on a shredding machine LabTest5.250SP1-VM. The material was loaded along the rolling direction of the base material and perpendicular to the weld. The average values of the yield strength, tensile strength and elongation are given in Tab. 5.

In the case of the sample without heat treatment and the sample subjected to artificial aging at a temperature of 150°C, all the test specimens were broken in the weld. In a sample whose artificial aging was performed at a temperature of 180°C, the test specimen broke at the weld site in only one case. In the other three test specimens, a fracture occurred in the base material.

From the measured strength characteristics, it is clear that the better mechanical properties are achieved in a sample whose artificial aging took place at a temperature of 150°C during a time of 24 hours.

5 DISCUSSION

The performed experiment was focused on determining the effect of heat treatment on resulting properties of welds prepared of AW2099 aluminium alloy. The aim of the experiment was to determine the effect of artificial aging temperature at a constant aging time of 24 hours. The AW2099 aluminium alloy was laser welded and then the welds were subjected to solution annealing for 1.5 hours at 540°C during which dissolution of precipitates occurred to form a homogeneous solid alpha solution. After solution annealing artificial aging was applied at 150°C and 180°C for 24 hours.

Based on the macroscopic analysis of heat-treated welded joints, it was found that the welded joints have a significant heat-affected zone. In this heat-affected zone, the structure was changed and the texture after rolling, which the base material has retained, was removed. The average width of the welds at the root of the weld was around 1-2mm, the width of the weld was 3mm on the surface and the HAZ was approximately 1-2mm wide on both sides of the weld.

Microscopic analysis revealed that the base material was formed by elongated rolled grains, which is a consequence of hot rolling. Recrystallization took place in HAZ, resulting in the development of a fine-grained polyhedral structure in this zone. The weld metal was formed by a dendritic structure. From the boundary of the HAZ and WM towards the axis of the weld, it was possible to observe columnar grains whose growth has been oriented in the same direction as heat dissipation during welding. There was no significant influence of different modes of heat treatment on the resulting structure of welded joints. The difference could be observed only at heat-untreated sample in which the weld metal and the base material reacted differently during etching. This uneven etching may be due to fewer segregated precipitates along grain boundaries.

Microhardness measurement was performed on the examined samples, where the measured values were compared with the values achieved for the sample without heat treatment. In the case of the sample which was not heat-treated, there was a significant decrease in the hardness in the area of the welded joint compared to the base material. This decrease in hardness in the weld metal was eliminated by applying artificial aging, which approximated the microhardness across the weld. When samples artificially aged at 150°C, the average hardness value of WM was 146.31 HV and BM 150.92 HV. This represents an increase in hardness of more than 36% compared to the hardness of the base material of the unheated sample, in the case of WM there was an increase in hardness of more than 86% after heat treatment. During artificial aging at 180°C, the average hardness value of WM was 101.05HV and BM 95.81HV. The sample aged for 24 hours at 180°C showed hardness approximately 34% lower than the sample aged for the same time at 150°C.

A static tensile test showed that the highest values of tensile strength and yield strength were obtained with a sample which was artificially aged at 150°C for 24 hours. The yield strength of this sample was approximately 427.27 MPa, which was 51% more than the strength of the unheated welded sample and 21% more than the strength of the sample, which was artificially aged at 180°C. The strength of the AW2099 alloy as delivered (446.50MPa) is 4% higher compared to the strength of the welded sample after artificial aging at 150°C (427.25MPa). The yield strength of a welded sample aging at 150°C was 390MPa, which is 30% more than the yield strength of an unheated welded sample (272.25MPa) and 38% higher than the yield strength of a welded sample aging at 180°C (239.75MPa). This yield strength (390MPa) is approximately 8% lower than the yield strength of AW2099 alloy as delivered (422.50MPa).

The static tensile test was performed 4 times for each heat treatment mode. In the case of a sample without heat treatment and a sample aging at a temperature of 150°C, the test specimen always broke at the weld site. In the case of a sample aging at 180°C, the test specimen broke at the weld site in only one case. There were pores in the welds, which could have influenced the results of the static test. The pores could have a notched effect in the static tensile test. This is also confirmed by the fact that in 9 cases out of 12 the test rod broke at the weld. For this reason, it would be good to use welding with filler material in the next experiment, or to focus on the preparation of materials before the welding process and to thoroughly remove surface oxides.

The experiment shows that the better mechanical properties of AW2099 weld joints were obtained after heat treatment after the welding process that consisted from solution annealing at 540° C for 1.5 hours followed by artificial aging at 150°C for 24 hours. Additionally, this mode of heat treatment is also more advantageous from an economic point of view.

6 CONCLUSIONS

The experiment was focused on determining the effect of heat treatment on resulting properties of the weld joints of AW2099 aluminium-lithium alloy. The aim of the experiment was to determine the effect artificial aging temperature at a constant aging time of 24 hours.

The AW2099 aluminium-lithium alloy was laser welded and then the weld joints were subjected to solution annealing for

1.5 hours at 540°C at which dissolution of precipitates occurred resulting in the formation of a homogeneous solid alpha solution. After solution annealing artificial aging was applied at the temperatures of 150°C and 180°C for 24 hours.
The experiment revealed that the better mechanical properties of AW2099 weld joints were obtained using the post-welding heat treatment consisted of the solution annealing at the temperature of 540°C for 1.5 hours followed by artificial aging at 150°C for 24 hours. This mode of heat treatment is more advantageous not only in terms of achieving better mechanical properties, but also from the economical point of view.

ACKNOWLEDGMENTS

The authors would like to thank the Slovak Research and Development Agency under contract no. APVV-15-0337 for providing financial support.

This publication was created thanks to the support of Fond of small projects in the framework of the call for non-repayable financial aid of program of co-operation Interreg V-A SK-CZ, number of the call: 5SK/FMP/11b for the project with title: „International Doctoral Seminar (IDS) as a support of development of international institutional partnerships “, contract number: SK/FMP/11b/05/002-Z.

REFERENCES

[Barta et al 2008] Barta, J., Maronek, M. (2008). Multimedialny sprievodca technologiou zvarania. Trnava: AlumniPress.

[Hrivnak 2009] Hrivnak, I. (2009). Zvaranie a zvaritelnost materialov. Bratislava: Slovenska technicka univerzita.

[Joshi 2005] Joshi, A. (2005). LITHIUM ALUMINIUM ALLOYS – The New Generation Aerospace Alloys. Retrieved from https://bit.ly/3A0l8uS

[Lin et al 2014] Lin, Y., Zheng, Z. Q, & Li, S. C. (2014). Effect of solution treatment on microstructures and mechanical properties of 2099 Al–Li alloy. Archives of Civil and Mechanical Engineering, 14(1), 61-71. https://doi.org/10.1016/j.acme.2013.07.005

[Michna et al 2005] Michna, S., Lukac, I., Ocenacek, V., Koreny, R., Drapala, J., Schneider, H. Miskufova, A. et al. (2005). Encyklopedie hliniku. Decin: Alcan Decin Extrusions.

[Moravcik et al 2018] Moravcik, R. et al. (2018). Kovove a nekovove materialy. Trnava: AlumniPress.

[MTF STU 2015] MTF STU. (2015). Laboratories of production technologies, metrology, assembly and materials. [online] Available from https://bit.ly/3D044qW

[Rioja et al 2012] Rioja, R. J., & Liu, J. (2012). The Evolution of Al-Li Base Products for Aerospace and Space Applications. Metallurgical and Materials Transactions A, 43, 3325-3337 https://doi.org/10.1007/s11661-012-1155-z

[Smiths Metal Centres 2018] Smiths Metal Centres. (2018). 2099 Technical Data sheet. Retrieved from https://bit.ly/3AULmAmWang, S., Huang, Y., & Zhao, L. (2018). Effects of different aging treatments on microstructures and mechanical properties of Al-Cu-Li alloy joints welded by electron beam welding. Chinese Journal of Aeronautics, 31(2), 363-369. https://doi.org/10.1016/j.cja.2017.07.002

CONTACTS:

Ing. Michaela Lopatkova
Slovak University of Technology in Bratislava, Faculty of Materials Science and Technology in Trnava
Jana Bottu 2781/25, 917 24 Trnava, Slovakia
E-mail: michaela.lopatkova@stuba.sk

Ing. Jozef Barta, PhD.
Slovak University of Technology in Bratislava, Faculty of Materials Science and Technology in Trnava
Jana Bottu 2781/25, 917 24 Trnava, Slovakia
E-mail: jozef.barta@stuba.sk

prof. Ing. Milan Maronek, CSc.
Slovak University of Technology in Bratislava, Faculty of Materials Science and Technology in Trnava
Jana Bottu 2781/25, 917 24 Trnava, Slovakia
E-mail: milan.maronek@stuba.sk

Ing. Matej Pasak, PhD.
Slovak University of Technology in Bratislava, Faculty of Materials Science and Technology in Trnava
Jana Bottu 2781/25, 917 24 Trnava, Slovakia
E-mail: matej.pasak@stuba.sk